LONG-TERM TREND OF DISSOLVED IRON CONCENTRATION AND HYDROLOGICAL MODEL INCORPORATING DISSOLVED IRON PRODUCTION MECHANISM OF THE AMUR RIVER BASIN

ONISHI T.[1], SHIBATA H.[2], NAGAO S.[2], PARK H.[2],
YOH M.[3] AND SHAMOV V.V.[4]
[1]*Research Institute for Humanity and Nature,* [2]*Hokkaido University*
[3]*Tokyo University of Agriculture and Technology*
[4]*Institute for Water and Ecological Problem, RAS*

1. INTRODUCTION

The Amur River is one of the largest trans-boundary river which runs through the boundary between China and Russia. The catchment area of the river is 2,050,057km^2 which is the nineth largest river in the world and the total length of the river is 4,350km. Thus, huge amount of fresh water is supplied by the Amur river to the Sea of Okhotsk (Ducklow et al., 2003). The Sea of Okhotsk is one of the most biologically productive regions in the world, and it supports high fisheries production. Recent studies show that dissolved iron plays an important role to maintain the biological productivity of the Sea of Okhotsk, and we suppose that one of the possible sources of dissolved iron is fresh water from the Amur river. Iron is an essential nutrient not only for the biological productivity of the Sea of Okhotsk but also for most biota. However, it is not well understood that how dissolved iron is produced and transported through the terrestial ecosystem.

This report consists of two parts. The first part is discussing about the characteristics of seasonal and inter-annual fluctuation of dissolved iron concentration in the Amur River basin. The second part is explaining about the structure of hydrological model which incorporates dissolved iron production mechanism. In addition, some simulated results are also shown. Last, perspective for future researches will be discussed.

2. TEMPORAL AND SPATIAL FLUCTUATION OF DISSOLVED IRON CONCENTRATION

Figure 1 is the long term dissolved iron concentration at Khabarovsk and Blagoveschensk. Sampling interval is not regular, but about 5 to 10 samples were collected in a year. The outstanding characteristics of fluctuating dissolved iron concentration is sharp increase during the period between 1996 and 1998 at Khabarovsk. Not the same acute increase during the same period was observed at Blagoveschensk, but relatively large increase tendency was also observed. Though the cause of this abrupt increase is not yet clarified, some possible reasons of increase will be discussed later. Another interesting aspect of change of dissolved iron concentration is that 10 to 15 years oscillation seems to exist. The first peak seems to occur during the early 1980s', and second peak is during late 1990s'.

Figure2 shows the monthly average during the period of 1960 to 1989 and the period of 1960 to 2006 at Khabarovsk and Blagoveschensk. The general characteristic of seasonal change is that highest concentration is recorded during the summer and early autumn season

(July to October). In addition, relatively high concentration is also observed during the winter season and spring season, especially in March and April. This tendency can be seen much clearer at the Blagoveschensk. And the same tendency can also be seen in the observed data in the Sanjiang plain (Yan et al. 2007). The mechanism of spring season increase of iron concentration is not yet clarified. One hypothesis is that biological process which is related to

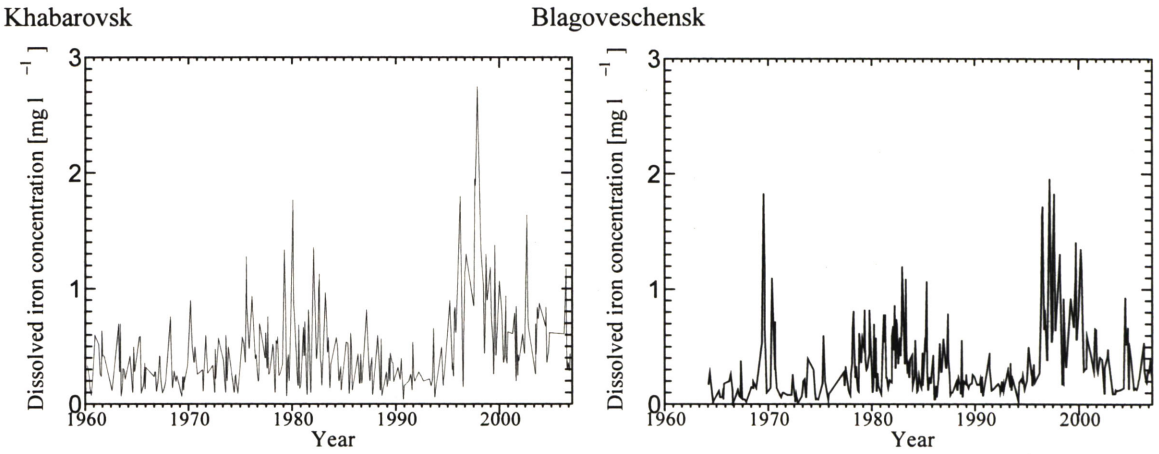

Figure1. Long term change of dissolved iron concentration at Khabarvosk and Blagoveschensk

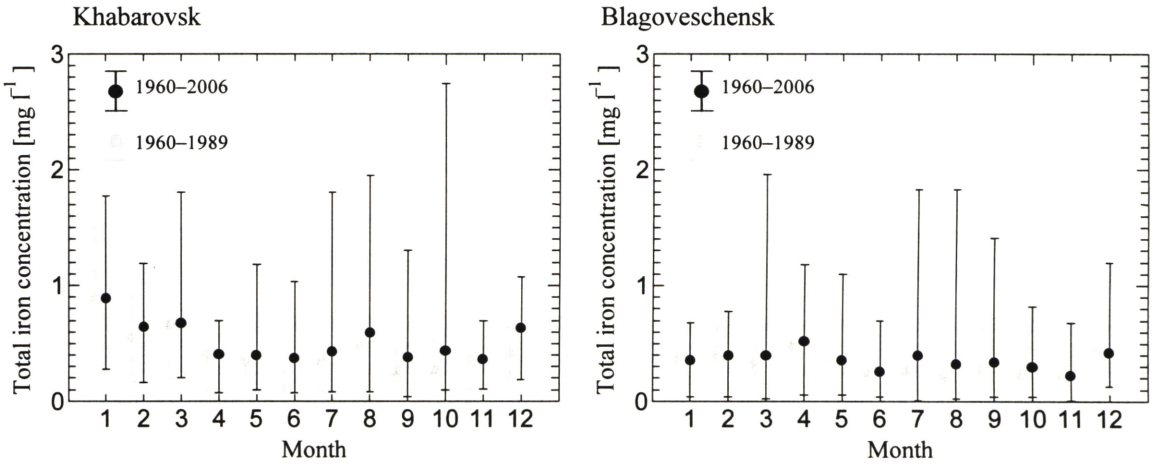

Figure2.Monthly average of dissolved iron concentration at Khabarvosk and Blagoveschensk

the soil freezing and thawing plays an important role in the phenomena.

To see the spatial trend and structure of dissolved iron concentration during the period of abrupt increase at Khabarovsk, the spatial fluctuation of dissolved iron concentration was analyzed. Figure3 shows the temporal change of dissolved iron concentration at the major tributaries which spread out in the Russian part of the Amur River basin. It seems that dissolved iron increase during the period between 1996 and 1998 is not localized phenomena, because increase trend can be observed at many observation stations. Combining with the observed data at Khabarovsk and Blagoveschensk, it can be deduced that spatially prevailing factors such as precipitation and temperature should be related.

Some possible factors which have a potential to control increases of dissolved iron concentration will be discussed in the rest of this section. Here we will consider precipitation and agricultural activity around Sanjiang plain. Figure4 shows the seasonal recipitation in (June-July-August) precipitation anomaly (climate value is calculated using the data during

the period of 1970-2000) in 1997. CRU TS2.0 data (Mitchell et al, 2004) are used for calculation. It can be observed that extremely large precipitation around Sanjiang plain was occurred. If we consider the amount of precipitation in each month in 1997, there was large August. On the other hand, Figure5 shows the temporal change of the numbers of wells in the

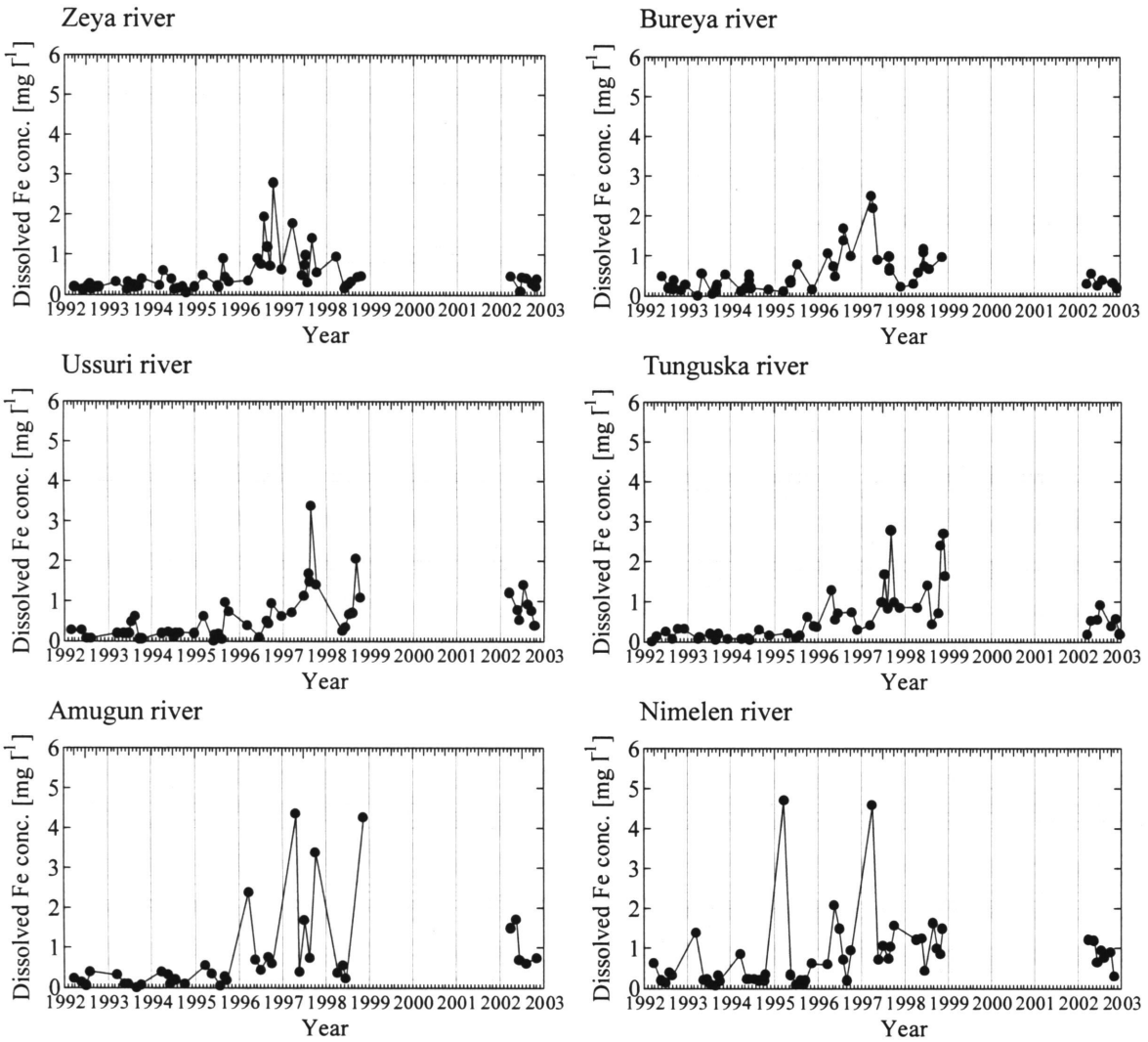

Figure 3 Change of dissolved iron concentration at the major tributaries of the Russian part of the Amur river basin during the period from 1992 to 1998 and 2002

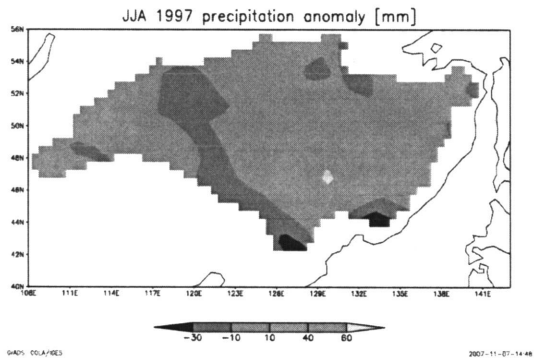

Figure4 Precipitation anomaly of during the period of JJA in 1997

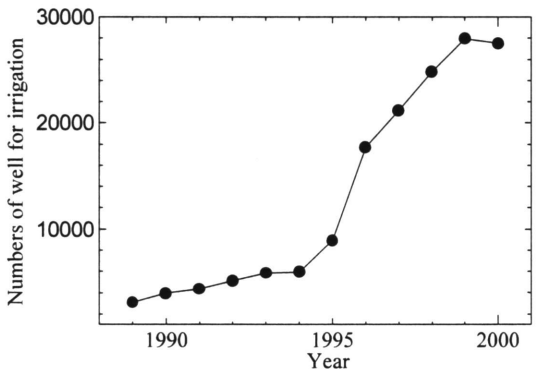

Figure5 Change of the numbers of irrigation wells in the three main national farmland in Sanjiang plain

3 national farmlands in the Sanjiang plain. Drastic increase of wells for irrigation was accelerated by conversion of dry lands to paddy fields during 1990s' (Park et al. 2001, Liu et al. 2002, Wang et al. 2006). As Yan et al. (2007) suggested, iron concentration of groundwater generally showed very high concentration larger than 10mg l^{-1}. Thus, if overflows from paddy fields occurred after a large precipitation, such water might contain highly concentrated iron. This is the one possible mechanism of high iron concentration during the late 1990s'. However, we have no clear evidence which supports this mechanism at now.

3. STRUCTURE OF HYDROLOGICAL MODEL

3.1 Concept of the model

The whole river basin is first divided into 0.5°x 0.5°grid. We consider each grid as one basin like usual Land Surface Model used in GCM. Discharge from each grid is calculated by using TOPMODEL concept as explained below. And discharge from grid is routed along the river network TRIP (Oki and Sud, 1998) shown in Figure6. Runoff routing process is calculated based on prescribed runoff velocity.

TOPMODEL that is frequently used in the hydrological modeling is one of the semi-distributed hydrolgoical models (Beven 1979, Beven 2001). Though many variations from the original version of TOPMODEL have been developed, the basic concept is not changed and effective. TOPMODEL concept was originally derived from a small scale catchment, the same concept is also used in the global scale LSMs such as MATSIRO (Takata et al., 2003).

In the model, each grid (0.5°x 0.5°) is again subdivided into 0.01°x 0.01°grid, and runoff from each subdivided grid is calculated. Schematic diagram of the model of each subdivided grid is shown in Figure7. The model consists of two parts. One is for dealing physical process which calculates runoff (TOP-RUNOFF), and the other is for dealing chemical process which calculates dissolved iron production (TOP-FE). The key concept in the model is that topographic index is related to the productivity of dissolved iron.

Figure 6 River network of the Amur river basin (TRIP)

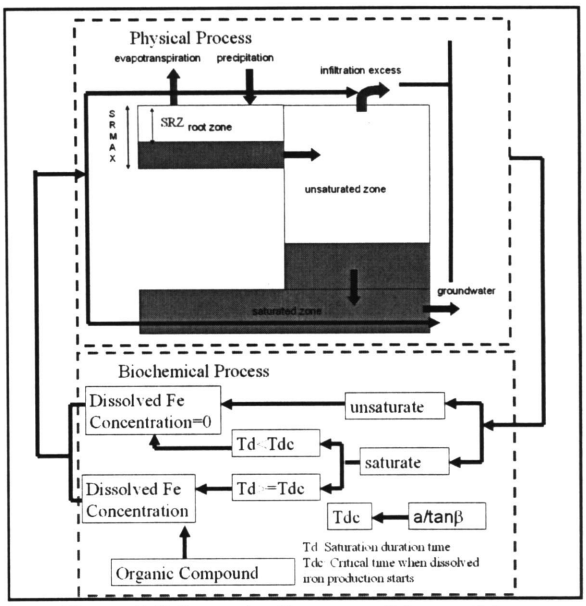

Figure7 Schematic diagram of the model

3.2 Topographic index and dissolved iron concentration

Based on the finding of relation between topographic index and dissolved iron concentration (Shibata et al. 2004, and Onishi 2007), we formulated the relationships between dissolved iron concentration and topographical index at each grid. Formula is constructed for wetland paddy fields and forest. For other land uses, it is assumed that there occurs no dissolved iron production. Figure8 shows the assumed relationships between topographic index and dissolved iron production at each grid. There must be other constraining factor of dissolved iron production such as dissolved organic carbon and annual precipitation.

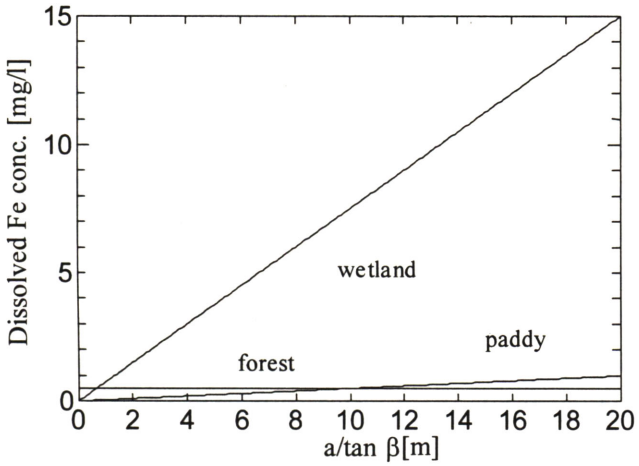

Figure8 Assumed relationships between topographic index and landuse type

3.3 Evapotranspiration

We used Penman-Monteith (Monteith, 1965) equaiton to calculate evapotranspiration rate as shown in the following equation.

$$\lambda_v E = \frac{\Delta(R_n + L - G) + \rho_a c_p (e_s - e_a) g_a}{\Delta + \gamma\left(1 + g_a / g_s\right)} \quad (1)$$

Here, E: evapotranspiration rate [mm d^{-1}], R_n: net shortwave radiation [W m^{-2}], L: net longwave radiation [W m^{-2}], G: soil heat flux [W m^{-2}]□ρ_a: density of dry air [kg m^{-3}], c_p: specific heat capacity of air [J kg^{-1} K^{-1}], e_s: saturated vapour pressure of the air temperature [Pa], e_a: vapour pressure of air [Pa], λ_v: latent heat of water vaporization [J kg^{-1}], Δ: rate of change of saturation vapor pressure with air temperature [Pa K^{-1}], γ: psychrometric constant [Pa K^{-1}], g_a: aerodynamic conductance [m s^{-1}], g_s: surface conductance [m s^{-1}], and, λ_v is set as 2.5 x 10^6,□γ□is set as 0.66.

3.4 Snow accumulation and melting

Before snow accumulation and melting, precipitation amount is divided into rainfall and snowfall according to the air temperature. An algorithm to divide precipitation into rainfall

and snowfall is shown in the following equation.

$$\begin{aligned} &Rain = P, T_a \geq T_{rain} \\ &Rain = P\frac{T_a - T_{snow}}{T_{rain} - T_{snow}}, Snow = P - Rain, T_{snow} < T_a < T_{rain} \\ &Rain = 0, Snow = P, T_a \leq T_{snow} \end{aligned} \tag{2}$$

Here, T_{rain} and T_{snow}: upper and lower threshold value of rainfall and snowfall division [K], T_a: mean daily air temperature [K]. In the snowpack melting process, our model adopted the simplest form of degree day method as shown in the next equation

$$M = F\max(0, T_a - T_F) \tag{3}$$

where M: melt rate as a water equivalent per unit area [LT^{-1}], F: degree-day factor [$LT^{-1}K^{-1}$], T: mean daily air temperature [K], and T_F: threshold temperature [K].

3.5 Data source and parameters

Stream flow data was obtained from two sources. One is Global Runoff Data Center (GRDC), and the other is from HYDROMET. Daily discharge amount of main stream of the Amur river is observed at Khabarovsk, Komsomo'lsk-Na-Amore and Bogorodskoy. The observed period is from 1940 to 1987 for Khabarovsk, 1940 to 2004 for Komsomo'lsk-Na-Amore and 1963 to 1987 for Bogorodskoy.

Climatic data which is needed for model simulation are net shortwave radiation, net long wave radiation, air temperature, wind velocity, specific humidity, and precipitation rate. In our analysis, we extracted these data from the National Centers for Environmental Prediction (NCEP) / National Centers for Atmospheric Research (NCAR) Reanalysis1 data sets. In generally, NCEP reanalysis2 data is reliable than reanalysis1 data. However, the main object of this research is to construct the framework of the model structure. Thus, in this analysis, we used the NCEP reanalysis1 data tentatively.

Land use and DEM data which are needed to calculate the dissolved iron productivity is compiled based on GIS data made by Pacific Institute of Geography (Ganzei et al., 2007). Hydraulic conductivity of each grid was made by linear interpolation of ISLSCP II data (Hall et al. 2005). Before running the model against the whole basin, various combinations of parameters were tested against several small sub-basins to select a reasonable parameter set which can roughly simulate runoff.

4. RESULTS AND DISCUSSION

4.1 Discharge

Figure 9 shows the observed and calculated discharge at Khabarovsk observation station from 1960 to 2002 with daily basis and monthly basis. It seems that seasonal trend of discharge can be simulated fairly well. However, discharge of summer season (from July to September) flood is generally under estimated. And, timing of peak in the simulated value is

faster than the observed value. These discrepancies between observed and calculated value is not peculiar, because one parameter set was applied to the whole river basin in spite of spatial variability of hydrological parameters. It can be said that we can simulate a rough trend of seasonal discharge despite of using only one parameter set.

To investigate the spatial distribution of discharge, observed value and calculated value at the several observation stations. Though there is a limitation of accuracy because of the lack of calibration data points, general characteristics of discrepancies between observed and calculated value is that discharge in the Songhua river basin is underestimate and discharge in the headwater area such as Amgun and Shilka basin is overestimate.

4.2 Dissolved iron concentration

Figure 10 shows the observed and calculated value of dissolved iron concentration at the Khabarovsk station. In general, the result of iron concentration in winter season is relatively good, but the increasing trend during the summer season can not be simulated. The reason of summer season discrepancy might be attributed to the processes the model considers. Hydrological processes which the model considers is basically the degree of soil saturation. Based on the saturation degree and the duration time of saturation, redox condition of each landuse is parameterized. However, there are additional two processes which must be

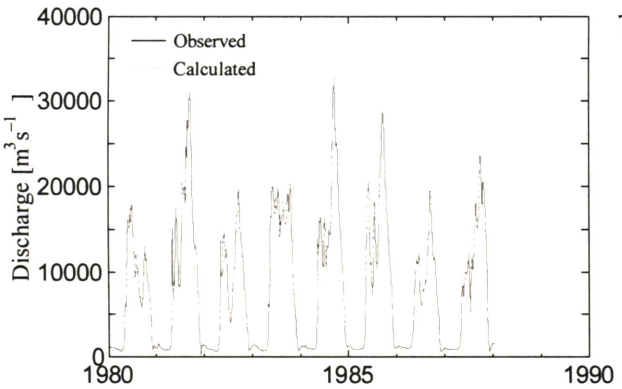

Figure 9 Comparison of discharge between observed observed and calculated value

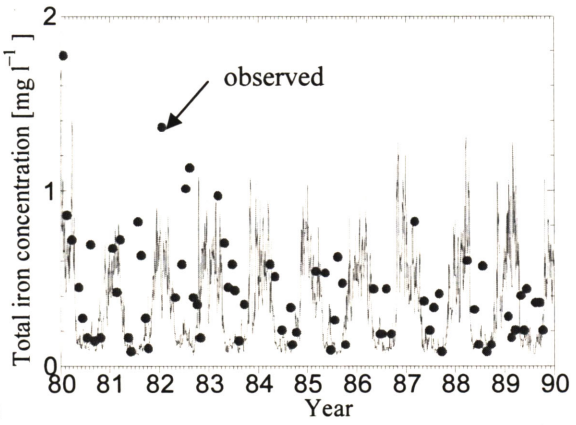

Figure10 Comparison of dissolved iron concentration between observed and calculated value

considered. One is increase of iron concentration in soils as the redox process proceeds. The other is the summer time flooding. Though it is suggested that flooding from rivers also plays a great importance to the iron transport from the findings of the project, the model does not consider the flooding process. Thus, it is suggested that flooding process must be incorporated in the m odel. In addition, the unknown mechanism of spring time increase is also not considered. This unveiled process might have less importance to the total dissolved iron flux in one year, because winter and spring time discharge is low.

5. SUMMARY AND FUTURE PERSPECTIVE

In this report, we first discussed about the characteristics of seasonal and inter-annual fluctuation of dissolved iron concentration in the Amur River basin. Through the analysis of

long-term iron concentration change at the Khabarovsk station, drastic increase during the period from 1996 to 1998 was found. Possible causes such as precipitation and agricultural activities were analyzed. However, mechanism of dissolved iron increase is not yet proved.

Next, structure of hydrological model which incorporates dissolved iron production mechanism was explained. And some simulated results were shown. Seasonal change of discharge at Khabarovsk station is relatively well simulated. However, peak discharge in summer time was underestimated and timing of the peak was obviously fast. If we looked into the detail of spatial variation of discharge, discharge of the Songhua River was underestimated. In addition, hydrological and chemical processes which must be incorporated into the model were discussed.

From the analysis of spatial variation of dissolved iron concentration during the period from 1992 to 1998, increasing trend of dissolved iron concentration was commonly observed. Thus, the increase of dissolved iron must have some relation to the large scale phenomena such as precipitation and temperature. Regression analysis between iron concentration and climate parameters is a future research task. Related to the model, first, optimization of hydrological parameters to improve the predicting accuracy of flood peak discharge amount in summer time is needed. Second, progress of redox process and flooding process must be incorporated into the model.

ACKNOWLEDGEMENT

We thank all researchers of IWEP for fruitful discussion and useful insights into the long term change of dissolved iron concentration. Analysis of this report largely owes to the continuous discharge data and iron concentration data which spans more than 40 years. Here, we are grateful to the HYDROMET of their effort for measuring discharge and water sampling and analyzing.

REFERENCE

Beven, K.J., Kirkby, M.J. (1979): A Physically-based variable contributing model of basin hydrology, Hydrolgical Science Bulletin, 24(1), pp.43-69

Beven ,K.J. (2001): Rainfall-runoff modeling the primer, John Wiley and Sons, pp.208

Ducklow, H.W., Oliver, J.L. and Smith Jr. W.O. (2003): The role of iron as a limiting nutrient for marine plankton processes, 'Interaction of the major biogeochemical cycles (Melillo, J.M., Field, C.B. and Moldan, B. Eds,)', Island Press, pp.295-310, Washington.

Ganzei S. S., Yermoshin V.V., Mishina N.V., Shiraiwa T. (2007): The basic features of land-use in the Amur River watershed, Report on Amur-Okhotsk Project No.4, Research Institute for Humanity and Nature, pp.139-150

Global Runoff Data Centre (GRDC): D-56068 Koblenz, Germany http://grdc.bafg.de/servlet/is/987/

Hall, Forrest G., G. Collatz, S. Los, E. Brown de Colstoun, D. Landis, eds. (2005): ISLSCP Initiative II. NASA. DVD/CD-ROM

Liu H., Zhang S., Lu X. (2002): Processes of wetland landscape changes in Naoli River basin since 1980s, J. Natural Resources, Vol17, No.6, pp.698-705 (In Chinese)

Monteith J.L. (1965): Evaporation and environment. In the state and movement of water in living organisms, Proceedings of the 19th Symposium, Society of Experimental Biology, Cambridge University Press, London

Mitchell, T.D., Carter, T.R., Jones, P.D., Hulme,M., New, M. (2003): A comprehensive set of high-resolution grids of monthly climate for Europe and the globe: the observed record (1901-2000) and 16 scenarios (2001-2100). Tyndall Centre Working Paper 55, pp.1-25

Oki T. and Y. C. Sud (1998): Design of Total Runoff Integrating Pathways (TRIP) - A global river channel network. Earth Interactions, 2, pp.1-37

Onishi T. (2007): Runoff properties of the Amur River and the construction of the hydrological model incorporating dissolved iron transport, Report on Amur-Okhotsk Project No.4, Research Institute for Humanity and Nature, pp.201-206

Park H., Sakashita A, Da Z., Yoshida K. (2001): Paddy development and national farm management in the Sanjiang plain: Case study conducted at theXinghua farm, The review of Agricultural Economics, Vol.57, Mar., pp.85-98

Shibata H., Konohira E., Satoh F. and Sasa K. (2004): Export of dissolved iron and the related solutes from terrestrial to stream ecosystems in northern part of Hokkaido, northern Japan, In, 'Report on Amur-Okhotsk Project: Proceedings of the Kyoto workshop 2004', Research Institute for Humanity and Nature, pp.87-92, Kyoto.

Takata K., Emori S., Watanabe T. (2003): Development of the minimal advanced treatments of surface interaction and runoff, Global and Planetary Change, Vol.38, pp.209-222

Wang Zongming, Zhang B., Zhang S., Li X., Liu D., Song K., Li J., Li F., Duan H. (2006): Changes of land use and of ecosystem service values in Sangjiang plain, Northeast China, Environmental monitoring and Assessment, Vol.112, pp.69-91

Yan B., Pan Y., Zhang B. Wang D. (2007): Distribution of dissolved iron in surface and groundwater in Sanjiang plain, Northeast China